

Inter-Cell Interference Coordination in Millimeter-Wave Cellular Networks

Haichao Wei*, Na Deng^{†‡}, Martin Haenggi[§]

*School of Information Science & Technology, Dalian Maritime University, Dalian, Liaoning, China

[†]School of Information & Communication Engineering, Dalian University of Technology, Dalian, Liaoning, China

[‡]National Mobile Communications Research Laboratory, Southeast University, Nanjing, 210096, China

[§]Department of Electrical Engineering, University of Notre Dame, Notre Dame, IN, USA

Email: *weihaichao@dlmu.edu.cn, ^{†‡}dengna@dlut.edu.cn, [§]mhaenggi@nd.edu

Abstract—In millimeter-wave (mm-wave) cellular networks, high-gain beamforming, realized with directional antenna arrays, is typically adopted to mitigate the severe propagation loss. However, the interference caused by such highly directional beams may, in turn, result in a significant number of transmission failures, especially for dense networks. To tackle this problem, we propose two inter-cell interference coordination (ICIC) schemes in mm-wave bands: one is merely based on the path loss incorporating the blockage effect (PL-ICIC); the other considers both path loss and directivity gain (PG-ICIC). To fully investigate the performance of both schemes, we first derive the exact expression for the success probability (reliability) of the typical user that is served. Secondly, to reflect the cost of interference coordination, we further derive the overall success probability taking into account that some users cannot be served due to limited resources. Numerical results show that both the proposed two schemes provide significant reliability improvements in the low signal-to-interference ratio (SIR) regime, in particular, the higher the number of antennas, the wider the range of SIR threshold for which there is an improvement. In addition, compared with PL-ICIC, PG-ICIC balances the available resources among all users well.

I. INTRODUCTION

Recently, millimeter wave (mm-wave) networks, operating at frequencies between 30 and 300 GHz, have attracted considerable attention from both academia and industry due to the wide available bandwidth and their potential to offer high data rates [1, 2]. Compared with conventional microwave communications, mm-wave communications have new characteristics, making the deployment and operation of mm-wave cellular networks more challenging. Firstly, because of the higher frequencies, mm-wave signals are susceptible to surrounding environments such as oxygen molecules and water vapor, which leads to significant path loss [3]. Secondly, due to the poor diffraction, mm-wave signals are more vulnerable to blockage by most solid materials, which limits the coverage region of mm-wave cellular networks. To overcome this limitation, mm-wave networks are envisioned to be densely deployed and use large antenna arrays (benefiting from the small wavelengths of the mm-wave band) to achieve acceptable coverage and rate [4]. However, as shown in [5], increasing the density of base stations (BSs) beyond a certain point leads to performance degradation, and the network tends to be interference-limited, i.e., the most important obstacle for successful transmission

is the high level of interference. To mitigate this problem, coordination among BSs has recently been recognized as a key requirement to effectively suppress the interference in dense mm-wave cellular networks [6–8].

An efficient approach to combat inter-cell interference is to exploit the cooperation between the multiple BSs. Generally, inter-cell interference coordination (ICIC) in conventional microwave networks is implemented through assigning different time/frequency/spatial dimensions to users that are severely impacted by the interference from adjacent cells and thus improves the per-user signal-to-interference-plus-noise ratio (SINR) performance [9–11]. However, since the mm-wave spectrum has several unique features such as high propagation loss, directivity, and sensitivity to blockage, the situation is different when ICIC is implemented in the mm-wave band. Regarding the interference characteristic, a key difference is that whether an interferer is dominant or not is not merely based on the distances or small-scale fading but on the actual power gains of the interfering beams and their LOS/NLOS states. As a result, the K -th strongest BS may not be the K -th closest BS. In this case, an effective ICIC scheme should be carefully designed to only coordinate those BSs that actually cause significant interference. Such a scheme, to our best knowledge, has not been studied in mm-wave cellular networks.

In this paper, we investigate the ICIC technique in mm-wave cellular networks considering the unique characteristics (i.e., the blockage effect and the highly directional transmission) of mm-wave communications. Specifically, in this paper, two ICIC schemes are proposed to improve the quality of experience for users: one is to mute the neighbor BSs merely based on the path loss incorporating the blockage effect (PL-ICIC); the other is to mute the neighbor BSs jointly considering the path loss and the directional array gain (PG-ICIC). Using stochastic geometry, we analyze the success probability and the overall success probability to reflect the reliability performance of the users served by their BSs and the overall users, respectively, where the latter one captures the ICIC cost. Numerical results demonstrate that while both ICIC schemes yield significant performance gain in terms of the success probability over no ICIC, especially in the low SIR regime, where PL-ICIC is better than PG-ICIC. From

the perspective of the overall success probability, PL-ICIC is worse than PG-ICIC and no ICIC because the muting operation based on the path loss leads fewer users to be served, while PG-ICIC achieves better overall performance than no ICIC with suitable coordination parameter setting, and thus balances the available resources among all users well.

II. SYSTEM MODEL

A. Network Model

We consider a mm-wave cellular network where a homogeneous Poisson point process (PPP) $\hat{\Phi}$ with density λ is used to model the location of the base stations (BS). We consider the pertinent properties of mm-wave communications such as directional beamforming of antenna arrays and blockage effects of the propagation environment. Each BS is assumed to be equipped with a uniform linear array (ULA) with N antenna elements, and a generalized LOS ball model [12] is adopted to capture the blockage effect. Specifically, all BSs apply analog beamforming with the assumption of perfect beam alignment. Letting w_m be the half-power beamwidth (HPBW), we consider a normalized flat-top antenna pattern, given by

$$G(\varphi) = \begin{cases} G_m & \text{if } |\varphi| \leq w_m \\ G_s & \text{otherwise,} \end{cases} \quad (1)$$

where $\varphi = \frac{d_t}{\rho} \cos \phi$ is the cosine direction corresponding to the angle of departure (AoD) ϕ of the transmit signal, which is termed the *spatial AoD*, with d_t and ρ representing the antenna spacing and wavelength, respectively. $d_t = \frac{\rho}{2}$ is assumed to enhance the directionality of the beam and avoid grating lobes; φ is assumed to be uniformly distributed in $[-0.5, 0.5]$. It is known from [13] that the actual antenna pattern of the ULA is

$$G_{\text{act}}(\varphi) = \frac{\sin^2(\pi N \varphi)}{N \sin^2(\pi \varphi)}, \quad (2)$$

and we have $G_m = N$, $G_{\text{act}}(w_m) = \frac{N}{2}$ and $G_s = \frac{1-2w_m G_m}{1-2w_m}$.

In the generalized LOS ball model, the LOS probability of the channel between two nodes with separation d is

$$P_{\text{LOS}}(d) = p_L \mathbf{1}_{d < R}, \quad (3)$$

where R is the maximum length of a LOS channel, and $p_L \in [0, 1]$ is the LOS probability. Denote by α_L and α_N the path loss exponents for LOS and NLOS channels, respectively. The stationarity of the PPP lends itself to the analysis for the typical user located at the origin. We denote by $\ell(x) = |x|^{-\alpha_x}$ the random path loss function from x to the origin, where

$$\alpha_x = \begin{cases} \alpha_L & \text{w.p. } P_{\text{LOS}}(|x|) \\ \alpha_N & \text{w.p. } 1 - P_{\text{LOS}}(|x|), \end{cases} \quad (4)$$

and all $\ell(x)_{x \in \hat{\Phi}}$ are independent.

Due to the blockage effect, the signal strength from the interferers outside the LOS ball is negligible because of the severe path loss over the large distance (at least R) [14]. Hence, the coverage analysis for the typical user can be restricted to a finite network region, and the relevant BSs, denoted by Φ , correspond to the PPP in a disk of radius

R centered at the origin. The BSs in Φ can be partitioned into two classes, where the BSs with LOS propagation to the typical user form a PPP Φ_L with density $\lambda_L = p_L \lambda$, while Φ_N with density $\lambda_N = p_N \lambda$ is the BS set with NLOS propagation, where $p_L + p_N = 1$ such that $\Phi = \Phi_L \cup \Phi_N$. In addition, Nakagami fading is adopted to model the small-scale fading, and LOS and NLOS paths have different parameters $M_L, M_N \in \mathbb{N}$. The power fading coefficient between node $x \in \Phi$ and the origin is denoted by h_x , which follows a gamma distribution $\text{Gamma}(M, \frac{1}{M})$ with $M \in \{M_L, M_N\}$, and all h_x are mutually independent and also independent of Φ .

B. Proposed ICIC Schemes

The typical user has a single antenna and is served by the BS with the smallest path loss, i.e., the serving BS x_0 satisfies

$$x_0 = \arg \min \{x \in \Phi : |x|^{-\alpha_x}\}. \quad (5)$$

Consider an interference-limited scenario with dense deployments, where the noise has little impact compared to the aggregated interference [14], and thus the transmit power of the BSs can be set to be unit power. The SIR at the typical user is

$$\text{SIR} \triangleq \frac{G_m h_{x_0} |x_0|^{-\alpha_{x_0}}}{\sum_{x \in \Phi^!} G(\varphi_x) h_x \ell(x)}, \quad (6)$$

where $\Phi^! = \Phi \setminus \{x_0\}$ and $G(\varphi_x)$ follows from (1). As in [14], the spatial AoD φ_x from an interferer to the typical user is uniformly distributed in $[-0.5, 0.5]$. To improve the user experience, we consider two ICIC schemes as follows.

1) *Path loss-based ICIC (PL-ICIC)*: We assume the interfering BSs in the coordinating set Ω_{PL} are muting the resource blocks (RBs) assigned to the typical user, where

$$\Omega_{\text{PL}} = \{x \in \Phi^! : |x_0|^{-\alpha_{x_0}} < \rho |x|^{-\alpha_x}\}, \quad (7)$$

and $\rho \geq 1$ is a parameter that characterizes the coordination level. In this case, whether an interfering BS participates in the interference coordination depends on its path loss to the typical user, which is related to the blockage effect from interfering BSs to the typical user. Denote by $\chi_x \in \{0, 1\}$ whether BS x is transmitting at the RBs assigned to the typical user. In PL-ICIC, we have $\chi_x = 1 - \mathbf{1}_{x \in \Omega_{\text{PL}}}$. The SIR at the typical user is

$$\text{SIR}_{\text{PL}} = \frac{G_m h_{x_0} |x_0|^{-\alpha_{x_0}}}{\sum_{x \in \Phi^!} G(\varphi_x) h_x \chi_x \ell(x)}. \quad (8)$$

When $\rho = 1$, no ICIC occurs, and SIR_{PL} becomes (6).

2) *Path loss and array gain-based ICIC (PG-ICIC)*: Jointly considering the blockage effect and the directional array gain of the mm-wave communications, we assume the interfering BSs in the coordinating set Ω_{PG} are muting the RBs assigned to the typical user, where

$$\Omega_{\text{PG}} = \{x \in \Phi^! : G_m |x_0|^{-\alpha_{x_0}} < \rho G(\varphi_x) |x|^{-\alpha_x}\}. \quad (9)$$

In PG-ICIC, we have $\chi_x = 1 - \mathbf{1}_{x \in \Omega_{\text{PG}}}$. The SIR at the typical user is

$$\text{SIR}_{\text{PG}} = \frac{G_m h_{x_0} |x_0|^{-\alpha_{x_0}}}{\sum_{x \in \Phi^!} G(\varphi_x) h_x \chi_x \ell(x)}. \quad (10)$$

When $\rho = 1$, no ICIC occurs, and SIR_{PG} also reverts to (6).

III. PERFORMANCE ANALYSIS

In this section, we first give the association probabilities and the distributions of the serving distances to the LOS/NLOS BSs to assist performance analysis of the two ICIC schemes. Then we give the exact results on the success probability for the typical user and overall success probability for all users.

Lemma 1. *The probabilities that $x_0 \in \Phi_k, k \in \{L, N\}$, are*

$$A_k = \pi \lambda_k \int_0^{R^2} \exp\left(-\pi \sum_{i \in \{L, N\}} \lambda_i r^{\alpha_k / \alpha_i}\right) dr. \quad (11)$$

Lemma 2. *Given that the typical user is associated with a LOS/NLOS BS, the probability density function (PDF) of the distance $r_0 = |x_0|$ between the typical user and its serving BS is $f_k(r)/A_k, k \in \{L, N\}$, where*

$$f_k(r) = 2\pi \lambda_k r \exp\left(-\pi \sum_{i \in \{L, N\}} \lambda_i r^{2\alpha_k / \alpha_i}\right). \quad (12)$$

The proofs of Lemma 1 and 2 are analogous to those of [15, Lemma 1 and 3] and are omitted from this paper.

A. Success Probability of the Typical Served User

The success probability is defined as the complementary cumulative distribution function (CCDF) of the SIR, given by

$$P(\theta) = \mathbb{P}(\text{SIR} > \theta), \quad (13)$$

where θ is target SIR threshold. The success probability can be thought of equivalently as the probability that the typical user achieves a target SIR θ , or the fraction of users who achieve an SIR of θ in any time slot in any realization of the PPP, which reflects the reliability performance of users served by their BSs. Since the desired signal link is either LOS or NLOS, the success probability is obtained by using the total probability law, expressed as

$$P(\theta) = A_L P_L(\theta) + A_N P_N(\theta), \quad (14)$$

where P_L and P_N are the success probabilities conditioned on the event that the desired link is LOS and NLOS, respectively. Our first result in this section is an exact expression of the success probability with the PL-ICIC scheme.

Theorem 1. *Letting $\epsilon_k = \frac{M_k}{G_m}$, the success probability $P(\theta)$ of the typical user with the PL-ICIC scheme is given by*

$$P(\theta) = \sum_{k \in \{L, N\}} \sum_{l=0}^{M_k-1} \int_0^R f_k(r) \frac{(-u)^l}{l!} \mathcal{L}_k^{(l)}(r, u)|_{u=\theta \epsilon_k r^{\alpha_k}} dr, \quad (15)$$

where $\mathcal{L}_k(r, u) = \exp(\eta_k(r, u))$, the superscript '(l)' stands for the l-th derivative of $\mathcal{L}_k(r, u)$ w.r.t u , and

$$\eta_k(r, u) = -2\pi \sum_{i \in \{L, N\}} \sum_{j \in \{m, s\}} \lambda_i \psi_j \phi\left(\bar{r}_{k,i}, \frac{G_j}{M_i}, \alpha_i, M_i\right), \quad (16)$$

where $\psi_m = 2w_m, \psi_s = 1 - \psi_m, \bar{r}_{k,i} = \min(R, \rho^{1/\alpha_i} r^{\alpha_k/\alpha_i})$ and

$$\phi(x, y, \alpha, m) = \int_x^R \left(1 - \frac{1}{(1+uyt^{-\alpha})^m}\right) t dt. \quad (17)$$

$\mathcal{L}_k^{(l)}(r, u)$ is given recursively by

$$\mathcal{L}_k^{(l)}(r, u) = \sum_{n=0}^{l-1} \binom{l-1}{n} \eta_k^{(l-n)}(r, u) \mathcal{L}_k^{(n)}(r, u), \quad (18)$$

where the n-th derivative of $\eta_k(r, u)$ w.r.t u follows as

$$\eta_k^{(n)}(r, u) = -2\pi \sum_{i \in \{L, N\}} \sum_{j \in \{m, s\}} \lambda_i \psi_j \phi^{(n)}\left(\bar{r}_{k,i}, \frac{G_j}{M_i}, \alpha_i, M_i\right), \quad (19)$$

and the n-th derivative of $\phi(\cdot)$ w.r.t u is

$$\phi^{(n)}(x, y, \alpha, m) = \frac{\Gamma(m+n)}{\Gamma(m)} \int_x^R \frac{(-y)^n t^{1-\alpha n}}{(1+uyt^{-\alpha})^{m+n}} dt. \quad (20)$$

Proof: See Appendix A.

Next, we give an exact expression of the success probability for the typical user with the PG-ICIC scheme.

Theorem 2. *The success probability $\tilde{P}(\theta)$ of the typical user with the PG-ICIC scheme is given by*

$$\tilde{P}(\theta) = \sum_{k \in \{L, N\}} \sum_{l=0}^{M_k-1} \int_0^R f_k(r) \frac{(-u)^l}{l!} \tilde{\mathcal{L}}_k^{(l)}(r, u)|_{u=\theta \epsilon_k r^{\alpha_k}} dr, \quad (21)$$

where $\tilde{\mathcal{L}}_k(r, u) = \exp(\tilde{\eta}_k(r, u))$, the superscript '(l)' stands for the l-th derivative of $\tilde{\mathcal{L}}_k(r, u)$ w.r.t u , and

$$\tilde{\eta}_k(r, u) = -2\pi \sum_{i \in \{L, N\}} \sum_{j \in \{m, s\}} \lambda_i \psi_j \phi\left(\tilde{r}_{k,i,j}, \frac{G_j}{M_i}, \alpha_i, M_i\right), \quad (22)$$

where $\tilde{r}_{k,i,j} = \min(R, \max(1, (\rho G_j / G_m)^{1/\alpha_i}) r^{\alpha_k/\alpha_i})$, and $\tilde{\mathcal{L}}_k^{(l)}(r, u)$ is given recursively similar to Theorem 1.

Proof: The proof is analogous to that of Theorem 1, with a modified spatial distribution of the interfering BSs according to the coordinating set Ω_{PG} . ■

Remark: Comparing Ω_{PL} and Ω_{PG} , we find that $\Omega_{PG} \subseteq \Omega_{PL}$, and thus the interference under the PG-ICIC scheme stochastically dominates that under the PL-ICIC scheme. As a result, we have $P(\theta) \geq \tilde{P}(\theta)$.

B. Overall Success Probability

Although both ICIC schemes improve the success probability of the typical user served by its BS, the muted BSs cannot transmit data at the RBs assigned to the typical user, and thus some users cannot be served by these muted BSs due to limited resources. Since the success probability of the typical user cannot capture this effect, we define a novel metric, termed *overall success probability*, that accounts for the fact that some users are no longer served. It is defined as

$$\xi(\theta) \triangleq \mathbb{E}\left[\frac{1}{1 + \zeta(r_0)} P(\theta | r_0)\right], \quad (23)$$

where r_0 is the link distance between the typical user and its serving BS, $\zeta(r_0)$ and $P(\theta | r_0)$ are the number of muted BSs and the success probability given r_0 , respectively. This definition captures the dependence between the number of

mutated BSs and the received SIR for users served by their BSs. Since $\Omega_{PG} \subseteq \Omega_{PL}$, we have $\zeta_{PL} \geq \zeta_{PG}$. Hence the higher success probability of the typical user served by its BS under the PL-ICIC scheme is achieved at the cost of fewer available RBs for neighboring BSs, which will lower the overall performance of the network. In the following, we analyze the overall success probability of both schemes.

Theorem 3. *The overall success probability of the PL-ICIC scheme is given by*

$$\xi(\theta) = \sum_{k \in \{L, N\}} \sum_{l=0}^{M_k-1} \int_0^R \frac{f_k(r) \omega_k(r) (-u)^l}{l!} \mathcal{L}_k^{(l)}(r, u) |_{u=\theta \epsilon_k r^{\alpha_k}} dr, \quad (24)$$

where

$$\omega_k(r) = \frac{1 - e^{-\pi \sum_{i \in \{L, N\}} \lambda_i (\bar{r}_{k,i}^2 - \min(R^2, r^{2\alpha_k/\alpha_i}))}}{\pi \sum_{i \in \{L, N\}} \lambda_i (\bar{r}_{k,i}^2 - \min(R^2, r^{2\alpha_k/\alpha_i}))}. \quad (25)$$

Proof: See Appendix B.

Theorem 4. *The overall success probability of the PG-ICIC scheme is given by*

$$\tilde{\xi}(\theta) = \sum_{k \in \{L, N\}} \sum_{l=0}^{M_k-1} \int_0^R \frac{f_k(r) \tilde{\omega}_k(r) (-u)^l}{l!} \tilde{\mathcal{L}}_k^{(l)}(r, u) |_{u=\theta \epsilon_k r^{\alpha_k}} dr, \quad (26)$$

where

$$\tilde{\omega}_k(r) = \frac{1 - e^{-\pi \sum_{i \in \{L, N\}} \sum_{j \in \{m, s\}} \psi_j \lambda_i (\bar{r}_{k,i,j}^2 - \min(R^2, r^{2\alpha_k/\alpha_i}))}}{\pi \sum_{i \in \{L, N\}} \sum_{j \in \{m, s\}} \psi_j \lambda_i (\bar{r}_{k,i,j}^2 - \min(R^2, r^{2\alpha_k/\alpha_i}))}. \quad (27)$$

Proof: The proof is analogous to that of Theorem 3, with a modified spatial distribution of the interfering BSs according to the coordinating set Ω_{PG} . ■

Remark: The success probability of the typical user reflects the user-perceived performance if the user is served by its BS, while the overall success probability captures the overall performance, which takes into account that fewer users can be served if some BSs are muted in certain RBs.

IV. NUMERICAL RESULTS

In this section, we will present numerical results of the success probability and the overall success probability for mm-wave cellular networks with the two BS muting schemes. The default system parameters are $\lambda = 5 \times 10^{-3}$, $p_L = 0.5$, $R = 300$, $M_L = 4$, $M_N = 2$, $\alpha_L = 2.5$, and $\alpha_N = 4$.

Fig. 1 compares the two ICIC schemes in terms of the success probability with different ρ and antenna size N . It is observed that the PL-ICIC scheme outperforms the PG-ICIC scheme in all cases. We also observe that the performance gap between the two ICIC schemes becomes larger when ρ or N become larger. For instance, when $N = 32$, the horizontal gaps between the two schemes with $\rho = 5$ and $\rho = 25$ are 0.3

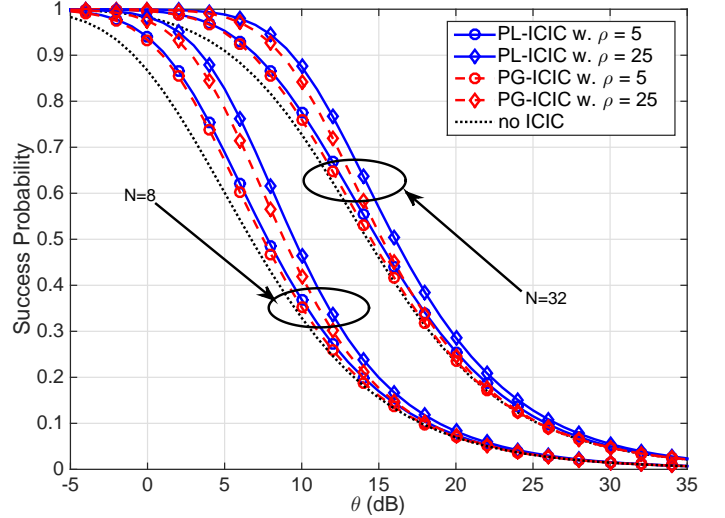


Fig. 1. The success probabilities for different ICIC schemes.

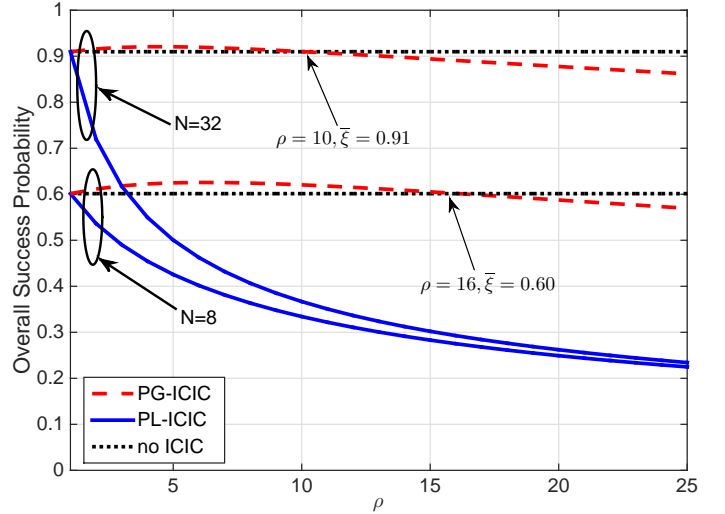


Fig. 2. The overall success probabilities for different ICIC schemes.

dB and 0.8 dB, respectively, and when $\rho = 25$, the horizontal gaps between the two schemes with $N = 8$ and $N = 32$ are 0.6 dB and 0.8 dB, respectively. This is because larger ρ and N magnify the area gap between the coordinating regions Ω_{PL} and Ω_{PG} and thus lead to a corresponding performance gap. It can be seen that the performance gain of both ICIC schemes over no ICIC becomes larger as θ decreases, which shows the advantage of the ICIC scheme in the low SIR regime. The higher the number of antennas, the wider the range of θ for which there is an improvement. For instance, when $N = 8$, there is performance improvement for $\theta < 20$ dB, and when $N = 32$, for $\theta < 30$ dB.

Fig. 2 shows the impact of the antenna size N and coordination parameter ρ on the overall success probability with $\theta = 5$ dB. We observe that the overall success probability of the PG-ICIC scheme outperforms that of the PL-ICIC scheme in both cases. As ρ increases, the overall success probability of the PL-ICIC scheme is always lower than that of no ICIC

and becomes smaller, while that of the PG-ICIC scheme first increases to a peak value and then declines. Hence, for a certain range of ρ , the PG-ICIC scheme is better than no ICIC in terms of overall success probability. These observations show the advantage of the PG-ICIC scheme on the overall network performance. It is also seen that a larger N leads to a larger overall success probability for both schemes, where N has a strong effect on the PG-ICIC scheme but only a slight effect on the PL-ICIC scheme.

V. CONCLUSIONS

In this paper, we proposed two ICIC schemes for mm-wave cellular networks, where the coordinating BSs are muted with the consideration of the unique characteristics (blockage effect and directional transmission) of mm-wave communications. To fully characterize the ICIC technique in mm-wave cellular networks, we provided analytical expressions of the performance metrics in terms of success probability and overall success probability with the aid of stochastic geometry. Numerical results demonstrate that the proposed two ICIC schemes significantly improve the success probability of the users served by their BSs for mm-wave networks. Meanwhile, the PL-ICIC scheme yields a better success probability than PG-ICIC scheme with more coordinated BSs muted and thus leads to worse overall success probability. Hence, the PL-ICIC scheme is suitable in scenarios with ultra-high reliability requirements and light load while the PG-ICIC scheme is effective in the scenarios with medium/high-reliability and heavy load.

ACKNOWLEDGMENT

The work of H. Wei has been supported by the Fundamental Research Funds for the Central Universities (3132019220). The work of N. Deng has been supported by the National Natural Science Foundation of China under Grant 61701071, by the China Postdoctoral Science Foundation (2017M621129 and 2019T120204), the open research fund of National Mobile Communications Research Laboratory, Southeast University (No. 2019D03), the Fundamental Research Funds for the Central Universities (DUT19RC(4)014). The work of M. Haenggi has been supported by the US NSF grant CCF 1525904.

APPENDIX A PROOF OF THEOREM 1

Proof: Letting $I = \sum_{x \in \Phi^1} G(\varphi_x) h_x \chi_x \ell(x)$, the success probability of PL-ICIC is given by

$$\begin{aligned} P_{\text{PL}}(\theta) &= \sum_{k \in \{\text{L}, \text{N}\}} A_k \mathbb{P} \left(\frac{G_m h_{x_0} r_0^{-\alpha_k}}{I} > \theta \right) \\ &= \sum_{k \in \{\text{L}, \text{N}\}} A_k \mathbb{E} \left[\tilde{\Gamma} \left(M_k, \theta \epsilon_k r_0^{\alpha_k} I \right) \right] \\ &= \sum_{k \in \{\text{L}, \text{N}\}} A_k \sum_{l=0}^{M_k-1} \mathbb{E} \left[e^{-\theta \epsilon_k r_0^{\alpha_k} I} \frac{(\theta \epsilon_k r_0^{\alpha_k} I)^l}{l!} \right] \end{aligned}$$

$$= \sum_{k \in \{\text{L}, \text{N}\}} \sum_{l=0}^{M_k-1} \int_0^R f_k(r) \frac{(-u)^l}{l!} \mathcal{L}_k^{(l)}(r, u) \Big|_{u=\theta \epsilon_k r^{\alpha_k}} \text{d}r,$$

where $\tilde{\Gamma}(x, y) = \Gamma(x, y)/\Gamma(x)$ is the normalized incomplete gamma function, $\mathcal{L}_k(r, u) = \mathbb{E}[e^{-uI}]$ is the Laplace transform of I under the condition that the serving BS x_0 is at a distance r and x_0 is LOS ($k = \text{L}$) or NLOS ($k = \text{N}$), and the superscript (m) stands for the m -th derivative of $\mathcal{L}_k(r, u)$ w.r.t u . The spatial distributions of interferers are different in two cases that the serving BS is either LOS or NLOS, which affects $\mathcal{L}_k(r, u)$. When $x_0 \in \Phi_{\text{L}}$ and $x_0 = r$, the interference powers from LOS and NLOS BSs are expressed as

$$\begin{aligned} I_{\text{L}}(r) &= \sum_{x \in \Phi_{\text{L}}} G(\varphi_x) h_x \chi_x |x|^{-\alpha_{\text{L}}}, \\ I_{\text{N}}(r) &= \sum_{x \in \Phi_{\text{N}}} G(\varphi_x) h_x \chi_x |x|^{-\alpha_{\text{N}}}. \end{aligned} \quad (28)$$

From Slivnyak's theorem [16], Φ_{L}^1 remains the same as the original PPP Φ_{L} . Then we have

$$\mathcal{L}_{\text{L}}(r, u) = \prod_{i \in \{\text{L}, \text{N}\}} \mathbb{E} e^{-u I_i(r)} = \prod_{i \in \{\text{L}, \text{N}\}} \mathcal{L}_{I_i}(r, u), \quad (29)$$

where $\mathcal{L}_{I_i}(r, u)$ follows as

$$\begin{aligned} \mathcal{L}_i(r, u) &= \mathbb{E} \left[\prod_{x \in \Phi_i} \left(\frac{1}{\left(1 + \frac{u G(\varphi_x) \chi_x |x|^{-\alpha_i}}{M_i}\right)^{M_i}} \right) \right] \\ &= \mathbb{E}_{\Phi_i} \left[\prod_{j \in \{\text{m}, \text{s}\}} \left(\frac{\psi_j}{\left(1 + \frac{u G_j \chi_x |x|^{-\alpha_i}}{M_i}\right)^{M_i}} \right) \right] \\ &\stackrel{(a)}{=} \exp \left(-2\pi \lambda_i \sum_{j \in \{\text{m}, \text{s}\}} \psi_j \int_{\bar{r}_{\text{L}, i}}^R \left(1 - \frac{1}{\left(1 + \frac{u G_j y^{-\alpha_i}}{M_i}\right)^{M_i}}\right) y \text{d}y \right) \\ &= \exp \left(-2\pi \lambda_i \sum_{j \in \{\text{m}, \text{s}\}} \psi_j \phi(\bar{r}_{\text{L}, i}, G_j/M_i, \alpha_i, M_i) \right), \end{aligned} \quad (30)$$

where step (a) follows from the probability generating functional (PGFL) of the PPP [16] and the lower integration limit is obtained since the closest interferer is at least at a distance $\bar{r}_{\text{L}, i} = \min(R, \rho^{1/\alpha_i} r^{\alpha_{\text{L}}/\alpha_i})$ obtained from the coordinating set Ω_{PL} . Letting

$$\eta_k(r, u) = -2\pi \sum_{i \in \{\text{L}, \text{N}\}} \sum_{j \in \{\text{m}, \text{s}\}} \lambda_i \psi_j \phi\left(\bar{r}_{k, i}, \frac{G_j}{M_i}, \alpha_i, M_i\right), \quad (31)$$

we have $\mathcal{L}_{\text{L}}(r, u) = \exp(\eta_{\text{L}}(r, u))$. Since $\mathcal{L}_{\text{L}}^{(1)}(r, u) = \eta^{(1)}(r, u) \mathcal{L}_{\text{L}}(r, u)$, $\mathcal{L}^{(l)}(r, u)$ can be calculated recursively according to the formula of Leibniz, given by

$$\mathcal{L}_{\text{L}}^{(l)}(r, u) = \sum_{n=0}^{l-1} \binom{l-1}{n} \eta^{(l-n)}(r, u) \mathcal{L}_{\text{L}}^{(n)}(r, u), \quad (32)$$

where the n -th derivative of $\eta_{\text{L}}(r, u)$ w.r.t u is

$$\eta_{\text{L}}^{(n)}(r, u) = -2\pi \sum_{i \in \{\text{L}, \text{N}\}} \sum_{j \in \{\text{m}, \text{s}\}} \lambda_i \psi_j \phi^{(n)}\left(\bar{r}_{k, i}, \frac{G_j}{M_i}, \alpha_i, M_i\right), \quad (33)$$

and the n -th derivative of $\phi(\cdot)$ w.r.t u is

$$\phi^{(n)}(x, y, \alpha, m) = \frac{\Gamma(m+n)}{\Gamma(m)} \int_x^R \frac{(-y)^n t^{1-\alpha n}}{(1+uyt^{-\alpha})^{m+n}} dt. \quad (34)$$

When $x_0 \in \Phi_N$ and $x_0 = r$, we derive $\mathcal{L}_N(r, u) = \exp(\eta_N(r, u))$ and its derivatives analogously. ■

APPENDIX B PROOF OF THEOREM 3

Proof: The overall success probability with the PL-ICIC scheme is

$$\xi(\theta) = \mathbb{E} \left[\frac{P_{\text{PL}}(\theta | r_0)}{1 + \zeta(r_0)} \right]. \quad (35)$$

Similar to the proof in Theorem 1, we have

$$\begin{aligned} \xi(\theta) &= \sum_{k \in \{L, N\}} A_k \sum_{l=0}^{M_k-1} \mathbb{E} \left[\frac{e^{-\theta \epsilon_k r_0^{\alpha_k} I} (\theta \epsilon_k r_0^{\alpha_k} I)^l}{1 + \zeta} \frac{1}{l!} \right] \\ &= \sum_{k \in \{L, N\}} \sum_{l=0}^{M_k-1} \int_0^R f_k(r) \underbrace{\mathbb{E} \left[\frac{1}{1 + \zeta} \mid r_0 = r \right]}_{\omega_k(r)} \\ &\quad \times \frac{(-u)^l}{l!} \mathcal{L}_k^{(l)}(r, u) \Big|_{u=\theta \epsilon_k r^{\alpha_k}} dr, \end{aligned} \quad (36)$$

where $\omega_k(r)$ characterizes the cost for coordinating the information transmission under the condition that $|x_0| = r_0$ and x_0 belongs to Φ_k , $k \in \{L, N\}$. Letting ζ_L and ζ_N be the number of the muted LOS and NLOS BSs, we have $\zeta = \zeta_L + \zeta_N$, and according to the desired BS belonging to LOS or NLOS, the following two disjoint events are considered.

One is conditioning on $x_0 \in \Phi_L$ and $|x_0| = r$. In this case, the LOS BSs $x \in \Phi_L$ are muted for the typical user under the PL-ICIC scheme if $r < |x| < \rho^{1/\alpha_L} r$ is satisfied, and thus ζ_L follows a Poisson distribution with mean $\mathbb{E}\zeta_L = \pi \lambda_L (\bar{r}_{L,L}^2 - r^2)$. A NLOS BS $x \in \Phi_N$ is muted if $r^{\alpha_L/\alpha_N} < |x| < \rho^{1/\alpha_N} r^{\alpha_L/\alpha_N}$ is satisfied, and ζ_N also follows a Poisson distribution with mean $\mathbb{E}\zeta_N = \pi \lambda_N (\bar{r}_{L,N}^2 - r^{2\alpha_L/\alpha_N})$. Given that $x_0 \in \Phi_L$ and $|x_0| = r$, ζ_L and ζ_N are independent, and thus ζ follows a Poisson distribution with mean

$$\mathbb{E}\zeta = \pi \sum_{i \in \{L, N\}} \lambda_i (\bar{r}_{L,i}^2 - r^{2\alpha_L/\alpha_i}), \quad (37)$$

and we further obtain

$$\begin{aligned} \omega_L(r) &= \sum_{n=0}^{\infty} \frac{1}{1+n} e^{-\mathbb{E}\zeta} \frac{(\mathbb{E}\zeta)^n}{n!} \\ &= \frac{e^{-\mathbb{E}\zeta}}{\mathbb{E}\zeta} \sum_{n=0}^{\infty} \frac{(\mathbb{E}\zeta)^{n+1}}{(n+1)!} \\ &= \frac{1 - \exp\left(-\pi \sum_{i \in \{L, N\}} \lambda_i (\bar{r}_{L,i}^2 - r^{2\alpha_L/\alpha_i})\right)}{\pi \sum_{i \in \{L, N\}} \lambda_i (\bar{r}_{L,i}^2 - r^{2\alpha_L/\alpha_i})}. \end{aligned} \quad (38)$$

The other is conditioning on $x_0 \in \Phi_N$ and $|x_0| = r$. In this case, ζ follows a Poisson distribution with mean

$$\mathbb{E}\zeta = \pi \sum_{i \in \{L, N\}} \lambda_i (\bar{r}_{N,i}^2 - \min(R^2, r^{2\alpha_N/\alpha_i})), \quad (39)$$

and $\omega_N(r)$ is derived analogously, given by

$$\omega_N(r) = \frac{1 - e^{-\pi \sum_{i \in \{L, N\}} \lambda_i (\bar{r}_{N,i}^2 - \min(R^2, r^{2\alpha_N/\alpha_i})}}{\pi \sum_{i \in \{L, N\}} \lambda_i (\bar{r}_{N,i}^2 - \min(R^2, r^{2\alpha_N/\alpha_i})}. \quad (40)$$

The final result is obtained by substituting (36), (38), (40) into (35). ■

REFERENCES

- [1] Z. Pi and F. Khan, "An introduction to millimeter-wave mobile broadband systems," *IEEE Communications Magazine*, vol. 49, no. 6, pp. 101–107, Jun. 2011.
- [2] F. Boccardi, R. W. Heath, A. Lozano, T. L. Marzetta, and P. Popovski, "Five disruptive technology directions for 5G," *IEEE Communications Magazine*, vol. 52, no. 2, pp. 74–80, Feb. 2014.
- [3] T. S. Rappaport, S. Sun, R. Mayzus, H. Zhao, Y. Azar, K. Wang, G. N. Wong, J. K. Schulz, M. Samimi, and F. Gutierrez, "Millimeter wave mobile communications for 5G cellular: It will work!" *IEEE Access*, vol. 1, pp. 335–349, 2013.
- [4] T. Bai and R. W. Heath, "Coverage and rate analysis for millimeter-wave cellular networks," *IEEE Transactions on Wireless Communications*, vol. 14, no. 2, pp. 1100–1114, Feb. 2015.
- [5] N. Deng and M. Haenggi, "A fine-grained analysis of millimeter-wave device-to-device networks," *IEEE Transactions on Communications*, vol. 65, no. 11, pp. 4940–4954, Nov. 2017.
- [6] C. Shi and G. Li, "Coordinated blanking for 5G millimeter-wave networks spectrum sharing," in *2016 IEEE 83rd Vehicular Technology Conference (VTC Spring)*, Nanjing, May 2016, pp. 1–5.
- [7] R. Kim, Y. Kim, and H. Lim, "Inter-BS interference-aware transmission coordination for millimeter wave networks," *IEEE Wireless Communications Letters*, vol. 6, no. 3, pp. 350–353, Jun. 2017.
- [8] J. Park, J. G. Andrews, and R. W. Heath, "Inter-operator base station coordination in spectrum-shared millimeter wave cellular networks," *IEEE Transactions on Cognitive Communications and Networking*, vol. 4, no. 3, pp. 513–528, Sep. 2018.
- [9] X. Zhang and M. Haenggi, "A stochastic geometry analysis of inter-cell interference coordination and intra-cell diversity," *IEEE Transactions on Wireless Communications*, vol. 13, no. 12, pp. 6655–6669, Dec. 2014.
- [10] J. Yoon and G. Hwang, "Distance-based inter-cell interference coordination in small cell networks: Stochastic geometry modeling and analysis," *IEEE Transactions on Wireless Communications*, vol. 17, no. 6, pp. 4089–4103, Jun. 2018.
- [11] 3GPP, "Evolved universal terrestrial radio access (E-UTRA):X2 application protocol (X2AP)," 3rd Generation Partnership Project (3GPP), Technical Specification (TS) 36.423, Sep. 2018, version 15.3.0.
- [12] S. Singh, M. N. Kulkarni, A. Ghosh, and J. G. Andrews, "Tractable model for rate in self-backhauled millimeter wave cellular networks," *IEEE Journal on Selected Areas in Communications*, vol. 33, no. 10, pp. 2196–2211, Oct. 2015.
- [13] C. A. Balanis, *Antenna Theory: Analysis and Design*. Hoboken, NJ, USA: John Wiley & Sons, 2005.
- [14] X. Yu, J. Zhang, M. Haenggi, and K. B. Letaief, "Coverage analysis for millimeter wave networks: The impact of directional antenna arrays," *IEEE Journal on Selected Areas in Communications*, vol. 35, no. 7, pp. 1498–1512, Jul. 2017.
- [15] H. S. Jo, Y. J. Sang, P. Xia, and J. G. Andrews, "Heterogeneous cellular networks with flexible cell association: A comprehensive downlink SINR analysis," *IEEE Transactions on Wireless Communications*, vol. 11, no. 10, pp. 3484–3495, Oct. 2012.
- [16] M. Haenggi, *Stochastic geometry for wireless networks*. Cambridge University Press, 2012.